Adv. Geosci., 20, 13–18, 2009
www.adv-geosci.net/20/13/2009/

Advances in Geosciences

Rain microstructure retrievals using 2-D video disdrometer and C-band polarimetric radar

M. Thurai[1], **V. N. Bringi**[1], **and W. A. Petersen**[2]

[1]Colorado State University, Fort Collins, Colorado, USA
[2]NASA-MSFC, Huntsville, Alabama, USA

Received: 29 August 2008 – Revised: 15 January 2009 – Accepted: 25 February 2009 – Published: 12 March 2009

Abstract. Measurements using the 2-D video disdrometer (2DVD) taken during a heavy rainfall event in Huntsville, Alabama, are analysed. The 2DVD images were processed to derive the rain microstructure parameters for each individual drop, which in turn were used as input to the T-matrix method to compute the forward and back scatter amplitudes of each drop at C-band. The polarimetric radar variables were then calculated from the individual drop contribution over a finite time period, e.g., 1 min. The calculated co-polar reflectivity, differential reflectivity, specific differential propagation phase and the co-polar correlation coefficient were compared with measurements from a C-band polarimetric radar located 15 km away. An attenuation-correction method based on the specific differential propagation phase was applied to the co-polar and differential reflectivity data from the C-band radar, after ensuring accurate radar calibration. Time series comparisons of the parameters derived from the 2DVD and C-band radar data show very good agreement for all four quantities, the agreement being sometimes better than the computations using the 1-min drop size distribution and bulk assumptions on rain microstructure (such as mean shapes and model-based assumptions for drop orientation). The agreement is particularly improved in the case of co-polar correlation coefficient since this parameter is very sensitive to variation of shapes as well as orientation angles. The calculations mark the first attempt at utilizing experimentally derived "drop- by-drop" rain microstructure information to compute the radar polarimetric parameters and to demonstrate the value of utilizing the 2-D video disdrometer for studying rain microstructure under various precipitation conditions. Histograms of drop orientation angles as well as the most probable drop shapes and the corresponding variations were also derived and compared with prior results from the 80 m fall "artificial rain" experiment.

Correspondence to: M. Thurai
(merhala@engr.colostate.edu)

1 Introduction

Polarimetric radar variables such as co-polar reflectivity (Z_h), differential reflectivity (Z_{dr}), specific differential propagation phase (K_{dp}) and co-polar correlation coefficient (ρ_{hv}) all depend fundamentally on the microstructure of hydrometeors within the radar pulse volume (see, for example, Bringi and Chandrasekar, 2001). For rain-filled media, the microstructure can be defined in terms of, (a) drop size distribution (DSD), (b) drop shape distribution, (c) drop orientations and, (d) fall velocities. It has been shown recently that the 2-D video disdrometer (2DVD) is capable of measuring all four quantities on an individual drop-by-drop basis (see Schönhuber et al., 2008). In this paper, we present such data taken during several rain events[1] in Alabama, USA, and compare the calculations made using these drop-by-drop data with C-band dual-polarimetric radar measurements. The radar used for this study is located in Huntsville, Alabama, 15 km from the 2DVD location.

2 Deriving drop orientation and shape

Schönhuber et al. (2008) have described the procedure for deriving drop shapes and drop orientation angles from the 2DVD images of individual hydrometeors. Moreover, Thurai et al. (2007) and Huang et al. (2008) have derived shape distributions and orientation angles (respectively) of drops from

[1]Under light-to-moderate wind speed conditions

Published by Copernicus Publications on behalf of the European Geosciences Union.

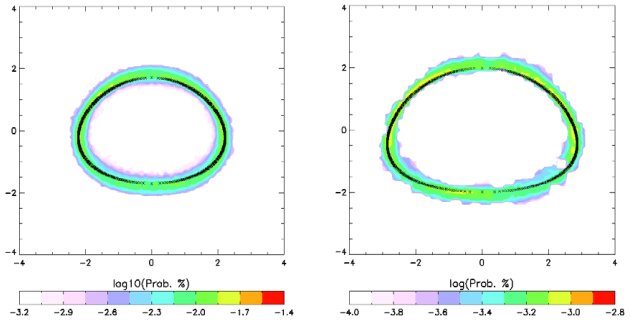

Fig. 1. Drop shapes in terms of probability for **(a)** D_{eq} in the range 4–4.25 mm (left) and **(b)** 5–5.25 mm (right), from several rain events in Alabama. The black line represents the "most probable" shape fitted using 2DVD data from the 80 m fall "artificial" rain experiment from Thurai et al. (2007). Note, the right hand plot shows for the first time the shape probability for the 5 mm drops, derived from 2DVD images of nearly 250 drops in natural rain.

an artificial rain experiment conducted under calm conditions where the drops were allowed to fall a distance of 80 m. Analysis of over 115 000 drops showed that the mean drop shapes could be fitted to a smoothed conical equation based on the equi-volumetric diameter, D_{eq}. Figure 1 shows the drop shapes derived from several rain events in Alabama and compares them with the fitted conical equation from the artificial rain experiment for D_{eq} in the interval, (a) 4–4.25 mm and (b) 5–5.25 mm. The colour scale in Fig. 1 represents the probability values and the finite width of the contour plots is indicative of the shape variations (due to, for example, drop oscillations). For the 5 mm case in Fig. 1b, there was sufficient number of drops (∼250) to derive the probable shape. Note that the fitted equation from the artificial rain experiment fits the Alabama data well, for both the 4 mm and the 5 mm drops. Smaller drop diameters (not presented here) also showed similar good agreement.

3 Analysis of one rain event

We now consider a single rain event in Alabama. The recorded 1minute DSD is shown as time series in Fig. 2a and the rainfall rate estimated from the DSD is shown in Fig. 2b. This event was chosen because of its wide range in the DSD, with significant numbers of large drops during certain time periods and because of the large variation in the rainfall rates ranging from a few mm h^{-1} to nearly 90 mm h^{-1}. In general, high rain rates are associated with a significant number of larger drops, for example, at the beginning of the event, drops in the 5–6 mm range are evident, and this corresponds to rainfall rates of over 60 mm h^{-1}.

The 2DVD images of each of the individual hydrometeors were processed to derive their shape, size and orientation, using the image de-skewing procedure described in Huang

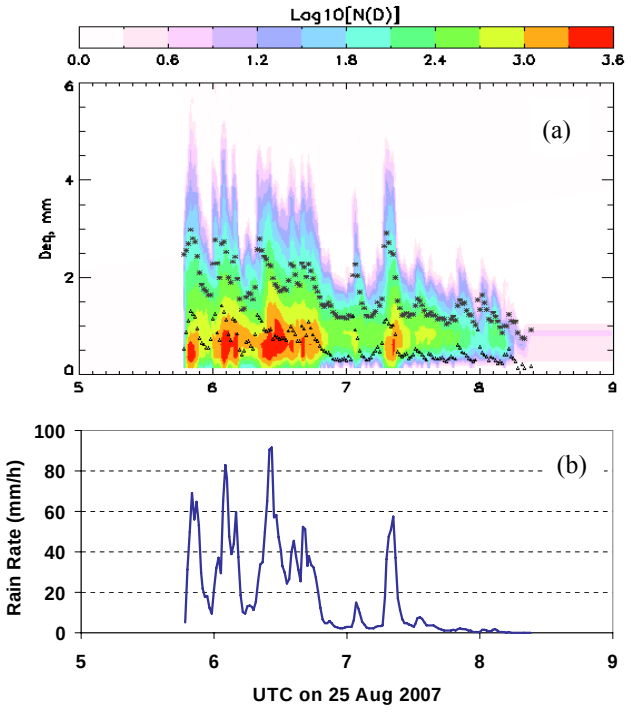

Fig. 2. **(a)** DSD time series of concentration (in $mm^{-1}\,m^{-3}$) as color intensity plot (log scale). The "solid triangle" marks depict the mass-weighted mean diameter (D_m) while the "star" marks depict the standard deviation or width of the mass spectrum (σ_M). **(b)** shows the rainfall rate (bottom panel) for the 25 August 2007 event, examined here in detail. This event was chosen because of the large range of rainfall rates.

et al. (2008). Figure 3a shows the combined distribution of the two canting angles derived from the two cameras. The distribution is symmetric with a near-zero skewness, and has a mean close to 0 deg. Its standard deviation is nearly 13 deg, which is larger than the 7.5 deg derived for the artificial rain experiment (conducted during low-wind wind conditions, as mentioned earlier).

When utilizing the T-matrix method for deriving the complex scattering amplitude of each hydrometeor, it is often conventional to define the orientation in terms of the polar (or zenith) angle and its local azimuth. Figure 3b and c show these two respective distributions corresponding to Fig. 3a. The same notation as Huang et al. (2008) is used here. As with the artificial rain experiment results, the zenith angle histogram corresponds to an expected Fisher distribution (Mardia, 1972), and the azimuth angle shows a near-uniform distribution from 0 to 360°. Note that the Fisher distribution is relevant to describing the statisitics of the orientation of the drop symmetry axis on a spherical surface (e.g., see Chapter 2 of Bringi and Chandrasekar, 2001). These histograms, together with the shape variations in Fig. 1a and b, imply that the orientation, size and shape of individual drops are being determined accurately by the 2DVD.

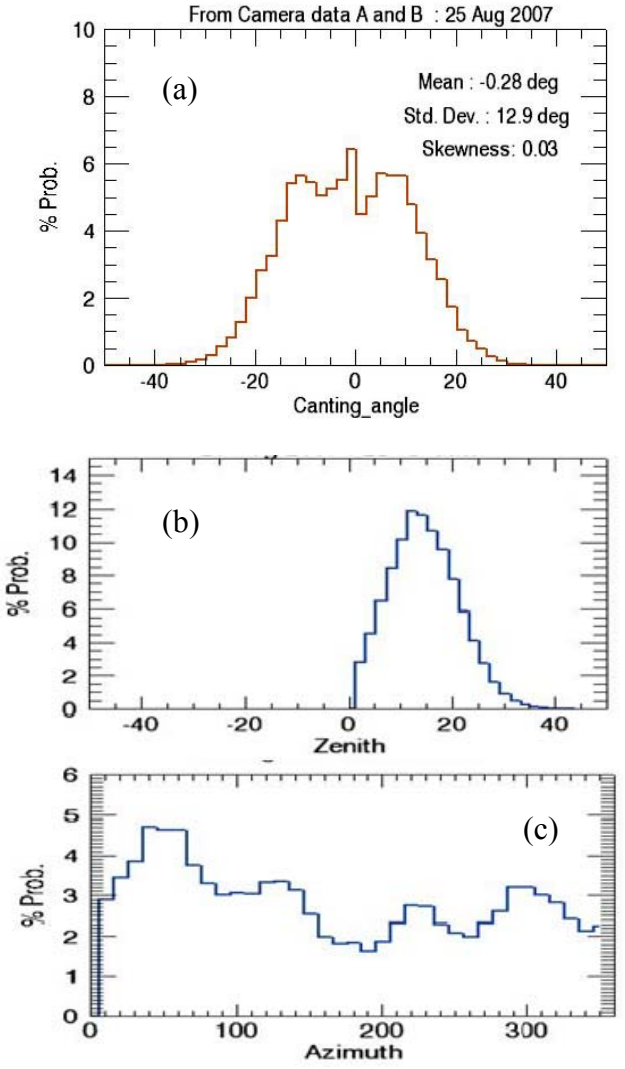

Fig. 3. **(a)** top panel, shows the canting angle distributions derived from individual drop images from both cameras (D>1.5 mm) using the de-skewing procedure (as described in Huang et al 2008) for the event on 25 August 2008, **(b)** the middle and **(c)** the lower panels show the corresponding zenith angle and the azimuth angle distributions, respectively. Note the azimuth angle shows a near-uniform distribution and the zenith angle shows the shape expected from a Fisher distribution.

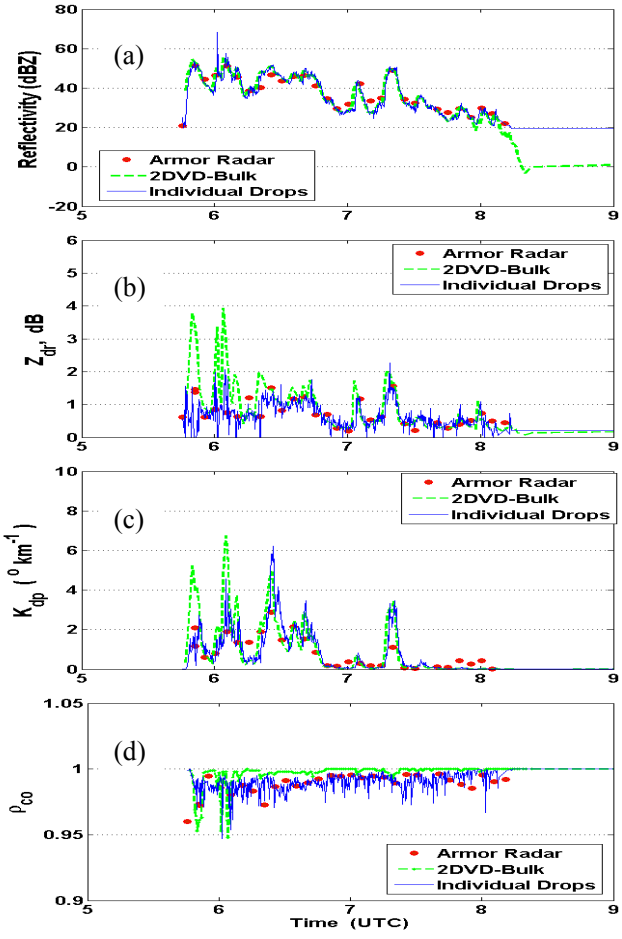

Fig. 4. Time series comparisons of **(a)** Z_h (top panel), **(b)** Z_{dr} (second panel), **(c)** K_{dp} (third panel) and **(d)** ρ_{hv} (last panel) for the 25 August 2007 event. In all cases, the blue line represents the calculations utilizing the individual drop information and the green line uses the 1-min integrated DSDs with bulk assumptions regarding drop shapes and orientations. The red dots show the C-band radar measurements (located 14.5 km away) extracted from operational PPI scans and, with weighted 9-point average over the 2DVD site.

4 Calculations of polarimetric radar variables

Based on the individual drop information, the 2×2 complex scattering matrix was derived using the T-matrix calculation procedure. The complex scattering amplitudes, in turn, were used to compute the four radar parameters, Z_h, Z_{dr}, K_{dp} and ρ_{hv} over a finite time period (1 min). Figure 4a, b, c and d show these (blue solid lines) as time series of the four radar quantities. Note that over each 1 min interval the total number of drops will vary, usually with rain rate. The 1-min averaging interval is a compromise between the larger sampling errors in the radar estimates if the averaging period is too small (∼tens of seconds) and the drop sorting errors if the averaging period is too large (>3 min). The latter has been discussed by Lee and Zawadzki (2005) while the former has been estimated for 2DVD by Schuur et al. (2001). The sampling errors in Z_h, Z_{dr} and K_{dp} for 1-min averaging of the 2DVD have been estimated to be around 1 dB, 0.25 dB, and 0.1 deg/km, respectively, which are reasonably consistent with the fluctuations in Fig. 4, yet the physical trends are readily discernible.

The "noisiness" of Z_{dr} and ρ_{hv} is due to both sampling errors as well as the physical sensitivity of these two quantities to the rain microstructure variations. Over-plotted as red dotted lines are the calculations using 1 min averaged DSDs

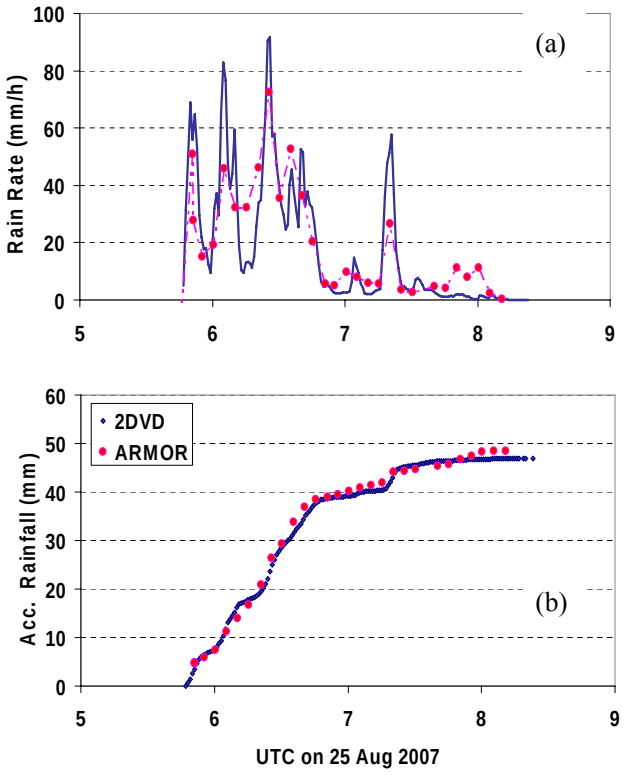

Fig. 5. Rainrate (top) and rain accumulation (bottom) comparisons between 2DVD data based estimates and those retrieved from the C-band polarimetric radar data.

and bulk assumptions regarding the shape and orientation of drops, namely that each drop has the "most probable" shape depending on its D_{eq} and that the drops have a symmetric canting angle distribution with zero mean and standard deviation of 7.5°. Whilst the reflectivity curves do not show much difference between the two cases, there are differences for the polarimetric radar parameters, as follows:

(a) the Z_{dr} and K_{dp} show significant differences at the beginning of the event

(b) ρ_{hv} shows differences throughout the event, with the drop-by-drop method giving noticeably lower and "noisier" values, except at the beginning of the event.

Note also that Z_h is not significantly different between the two methods, as would be expected since Z_h is relatively insensitive to axis ratio nor canting angle distributions. For Rayleigh scattering, most of the increase in Z_{dr} is actually due to a decrease in Z_v, with Z_h being approximately constant.

We now compare these calculations with actual C-band radar measurements.

5 Comparison with C-band measurements

The C-band polarimetric radar (ARMOR, see Petersen et al., 2007) used here for comparisons is an operational radar located 14.5 km from the 2DVD site. The antenna beamwidth is 1° and the range resolution is 250 m. The C-band data were corrected for co-polar and differential attenuation using K_{dp}-based algorithms, similar to the procedure described in Bringi et al. (2006), and the corrected Z_h and Z_{dr} as well as K_{dp} and ρ_{hv} were extracted at and around the 2DVD location (weighted 9-point average over three consecutive range gates and 3 azimuths centred around the 2DVD site). The areal averaging is over approximately 750×400 m. Determining an optimal area for radar averaging is very difficult since it depends on the spatial correlation structure of the particular variable such as Z or R. Bolen et al. (1998) have given a radar-gage based method of determining the optimal averaging cell. They found the decorrelation (1/e) distances of approximately 0.8–1 km for the events they analyzed. Thus our use of an averaging "cell" of 750 m in range and 3 azimuths is not unreasonable.

The averaged values extracted from the operational PPI sweeps, taken every 5 min, are included as red dots in Fig. 4. Clearly the agreement in the polarimetric parameters is much better with the drop-by-drop based calculations, particularly during the first hour of the event (see Appendix A for explanation), and demonstrates the importance of the rain microstructure parameters for calculating the radar parameters (and vice-versa).

In Fig. 5 we compare (a) rainfall rates and, (b) rain accumulation. The ARMOR-based rainfall rates were derived from a K_{dp}-based algorithm {R=22.9 $K_{dp}^{0.769}$ in mm/h for K_{dp}>0.01 deg/km}. The $R-K_{dp}$ relationship is based on a mean fit to the 2DVD data using the scattering calculations as explained in Sect. 4. The same applies to the D_m-Z_{dr} given later. The agreement between the two rain rates in Fig. 5 is good, considering that the 2DVD has an effective sensor area of 10 cm by 10 cm whereas the radar samples a much larger pulse volume (but nearly instantaneous). In addition, the smoothing of the differential propagation phase results in poorer spatial resolution of the K_{dp} especially in small intense cells with peak R values from the radar being lower than the 2DVD as evident in Fig. 5. The rain accumulation over the entire event shows very good agreement since the 'over/under' predictions tend to cancel out in the time integration. More importantly, the two estimates track each other very closely, both totaling around 46 mm of rainfall in a period of two and a half hours. However such comparisons need to be made over many events in order to validate the rain rate algorithm used herein.

Finally in Fig. 6 we compare the histograms of mass-weighted mean diameter, D_m, derived from a Z_{dr}-based algorithm {D_m=1.7824$Z_{dr}^{0.394}$ in mm} based on a single PPI sweep of ARMOR data up to 60 km in range, and from the drop-by-drop 2DVD data. The PPI was taken at 06:06 UTC,

i.e. during the passage of the rain cell over the 2DVD site. Note that the large number of radar resolution volumes (several hundreds) included in the histogram represents a wide range of D_0 values such that a convergent histogram is attained. The resolution volumes selected includes the area of the convective cell that is similar to that which traversed across the 2DVD site. This space-time "ergodic" principle, while being loosely applied here, is reasonable provided the radar estimates are based on an area of the convective cell which is not too dissimilar to that sampled at a different time by the 2DVD. Bringi et al. (2003) have used this idea to great advantage in arriving at a global statistics of the DSD variation of mean D_0 and mean N_0.

Once again, the two histograms lie close to each other, and, moreover, it is worth noting that the distribution is typical, on average, for sub-tropical convective rain events examined herein, that is mode of around 1.3 mm and a significant skewness with D_m values extending to more than 2.5 mm for a few percent in both cases. The average DSD characteristics of sub-tropical/tropical rain from a number of locations around the world is given in Bringi et al. (2003) based on both disdrometer and radar-based retrievals. The mean D_m from their sub-tropical/tropical cluster is in the range 1.5–1.7 mm (which is close to the mean of the histogram in Fig. 6). The good agreement between the two histograms in Fig. 6 is also one way of demonstrating the reliability of the Z_{dr}-based algorithm to derive D_m on a statistical basis.

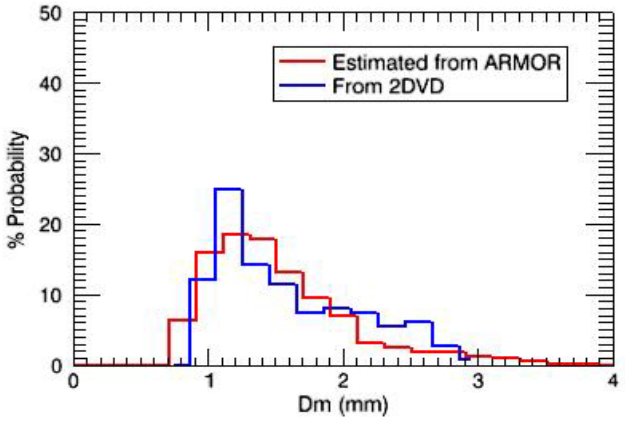

Fig. 6. Histogram of D_m from 2DVD for the entire event on 25 August 2007 compared with those estimated using a single PPI sweep of the C-band data. They are not only similar to each other but agree with the typical distributions expected for such sub-tropical convective rain events, with the mode at around 1.3 mm and a significant skewness towards the larger values.

6 Conclusions

Drop-by-drop measurements from the 2DVD have been demonstrated to provide pertinent information on rainfall microstructure required for deriving the polarimetric radar variables. When compared with simultaneous C-band radar observations, the calculations which utilize the microstructure data give closer agreement than those using bulk assumptions. The improvement in ρ_{hv} comparisons is particularly remarkable since assuming a mean shape versus drop diameter (D) relation does not capture the variance of shapes which tends to decorrelate the H and V received signals. We believe this is the first demonstration that drop-by-drop predictions of ρ_{hv} agree well with radar measurements. In the case of K_{dp}, the result is more strongly dependent on D_m rather than on the shape variations about the mean. For Z_{dr}, the drop-by-drop calculations become more important as the width of the axis ratio distribution increases with increasing D. In the case of Z_h, the drop-by-drop calculations, as expected, are not much different from using the bulk assumptions. We expect that for radars capable of measuring LDR, the drop-by-drop computations will be more important similar to what has been observed here with ρ_{hv}.

Rainfall rates, rain accumulation and D_m histograms were retrieved from the C-band PPI scans using a 'tuned' retrieval algorithm. These retrievals were consistent with those derived from the 2DVD.

Since the start of the observation campaign in Alabama, there have been nearly 50 rain events recorded by the 2DVD and by the ARMOR radar. Further analyses of these events will be carried out in order to develop/evaluate retrieval algorithms at C-band, with particular emphasis on high rainfall rates. Recent modeling studies (see Beard et al., 2008) indicate that collision-forced drop oscillations can occur in intense rain, in which case Z_{dr} and K_{dp} will be smaller than the expected values using standard shape models. Such hypotheses will be investigated using the Alabama dataset, as well as the possibility of including ρ_{hv} for improved DSD retrievals for such intense events (as was the case in Thurai et al., 2008).

Appendix A

Axis ratio distributions

In Fig. 4, we saw that, during the first hour of the event, the Z_{dr} calculated using the drop-by-drop method gave lower estimates than those calculated using the 1-min DSDs together with model based assumptions on drop shapes and orientations. We also saw that the agreement between the two estimates was much closer during the latter half of the event. The reason for this could be several, but the main cause is likely to be the "modified drop shapes" that were observed from the 2DVD data during the first hour of the event. Figure A1 shows the axis ratio distributions for the 3.5–3.75 mm drops (derived from the ratio of the maximum vertical chord to the maximum horizontal chord) for two time periods, viz.

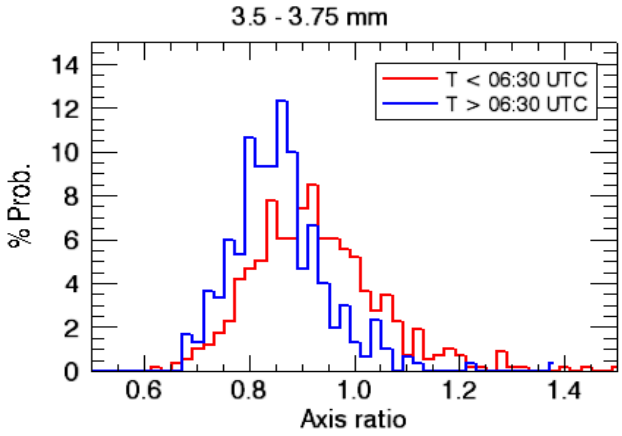

Fig. A1. Histograms of axis ratios for the 3.50–3.75 mm drop diameter range using the 2DVD data for the 25 August 2007 event in Alabama, prior to (in red) and after (blue) 06:30 UTC. Note the histogram after 06:30 UTC is very similar to the axis ratio distributions from the 80 m fall (artificial) rain experiment, whereas the histogram before 06:30 shows significantly higher axis ratios (relatively more spherical shapes) and a wider distribution.

before and after 06:30 UTC. The latter (i.e. the time period after 06:30 UTC) shows axis ratio distributions which are very similar to those found in the artificial rain experiment, with mean given by the fitted formula (Eq. 2 of Thurai et al., 2007):

$$\frac{b}{a} = 1.065 - \left[6.25 \times 10^{-2}\left(D_{eq}\right)\right] - \left[3.99 \times 10^{-3}\left(D_{eq}^{2}\right)\right] + \left[7.66 \times 10^{-4}\left(D_{eq}^{3}\right)\right] - \left[4.095 \times 10^{-5}\left(D_{eq}^{4}\right)\right]$$

for $D_{eq} \geq 1.5$ mm (A1)

which gives 0.815 for this drop diameter interval. This lies close to the mode of the histogram corresponding to the second half of the event, but is significantly lower than the histogram mode (∼0.9) during the first hour of the event.

The shift in the axis ratio distributions (for T <06:30 UTC) towards the less oblate ("more spherical") shapes would be expected to give rise to lower Z_{dr} and K_{dp} calculated using the drop-by-drop method. Since the ARMOR data also shows these lower values, it seems likely that the "more spherical shapes" do possibly represent mixed-mode oscillations (as in Beard et al., 2008). Such mixed mode oscillations can be either caused by collisional-forcing of drop oscillations and/or some component of spontaneous transverse oscillations. Note, however, this does not apply to the second half of the event (for T >06:30 UTC).

Acknowledgements. This work was funded by the National Science Foundation via grant ATM-0603720, NASA Grant NNX07AK39G (WAP), and NOAA Grant NA06-OAR4600156 (WAP et al.). We also wish to thank Günter Lammer and Michael Schönhuber (both from Joanneum Research, Austria) for help with the 2DVD software, and Christopher Shultz, Elise Johnson and Dustin Phillips (all from UAH) for help with the 2DVD installation and maintenance in Alabama, and to G.-J. Huang (CSU) for assistance with the T-matrix computations.

Edited by: S. C. Michaelides
Reviewed by: two anonymous referees

References

Beard, K. V., Bringi, V. N., Thurai, M., and Johnson, D. B.: Modeling and measurement of the shape of raindrops, Proceedings of the 5th European Radar Conference on Meteorology and Hydrology (ERAD 2008), Helsinki, Finland, paper 7.7, 2008.

Bolen, S., Bringi, V. N., and Chandrasekar, V.: An optimal area approach to intercomparing polarimetric radar rain rate algorithms with guage data, J Atmos. Oceanic Technol., 15, 605–623, 1998

Bringi, V. N. and Chandrasekar, V.: Polarimetric Doppler Weather Radar: Principles and Applications, Cambridge University Press, 636, 2001.

Bringi, V. N., Thurai, M., Nakagawa, K., Huang, G. J., Kobayashi, T., Adachi, A., Hanado, H., and Sekizawa, S.: Rainfall estimation from C-band polarimetric radar in Okinawa, Japan: Comparisons with 2D-video disdrometer and 400 MHz wind profiler, J. Met. Soc. Japan, 84, 705–724, 2006.

Huang, G-J., Bringi, V. N. and Thurai, M.: Orientation Angle Distributions of Drops after 80 m fall using a 2-D-Video Disdrometer, J. Atmos. Oc. Tech., 25, 1717–1723, 2008.

Lee, G.-W. and Zawadzki, I.: Variability of drop size distributions: Noise and Noise filtering in Disdrometric data, J. Appl. Met., 44, 634–652, 2005.

Mardia, K. V.: Statistics of Directional Data, Academic Press, New York, 1972.

Petersen, W. A., Knupp, K. R., Cecil, D. J., and Mecikalski, J. R.: The University of Alabama Huntsville THOR Center instrumentation: Research and operational collaboration, extended abstract P. 8A.8, 33rd Conf. on Radar Meteor., August 2007, Cairns, Australia, 2007.

Schönhuber, M., Lammer, G. and Randeu, W. L.: The 2-D-Video-Distrometer, Chapter 1 in: Precipitation: Advances in Measurement, Estimation and Prediction, edited by: Michaelides, S., Springer, 2008. ISBN: 978-3-540-77654-3, 2008.

Schuur, T. J., Ryzhkov, A. V.,. Zrnić, D. S., and Schoenhuber, M.: Drop size distributions measured by a 2-D video disdrometer: Comparison with Dual-polarization radar data, J. Appl. Met., 40, 1019–1034, 2001.

Thurai, M., Huang, G.-J., Bringi, V. N., Randeu, W. L., and Schönhuber, M.: Drop Shapes, Model Comparisons, and Calculations of Polarimetric Radar Parameters in Rain, J. Atmos. Ocean. Tech., 24(6), 1019–1032, 2007.

Thurai, M., Hudak, D., and Bringi, V. N.: On the Possible Use of Co-polar Correlation Coefficient for Improving the Drop Size Distribution Estimates at C-band, J. Atmos. Oc. Tech., 25, 1873–1880, 2008